Antisense oligonucleotides reverse SPTLC1-related hereditary sensory neuropathy in a mouse model

Jinhong Meng,[1,2] Shunyi Ma,[1] Museer A. Lone,[3] Hou Wang Lam,[1] Qiang Zhang,[1] Shuzhi Cheng,[1] Shona Mackie,[1] Emma Graham,[1] Hanna Kedzior,[1] Charalambos Demetriou,[1,4] Nicole Ziak,[3] Laura Andreoli,[5] Simon Beggs,[5] Stephanie Koch,[5] Alex J. Clark,[6] David L. Bennett,[7] Thorsten Hornemann,[3] Francesco Muntoni,[2,4,8] Mary M. Reilly[9] and Haiyan Zhou[1,2]

Abstract

Hereditary sensory neuropathy type IA (HSN1A) is a rare neurodegenerative condition caused by dominant mutations in the Serine Palmitoyl Transferase Long Chain base subunit 1 (SPTLC1) gene. There is no treatment available.

Allele-specific silencing by antisense oligonucleotides (ASOs) to preferentially silence the mutant transcripts has shown therapeutic promise for dominant gain-of-function genetic disorders. In this study, we validated an allele-specific ASO therapy to selectively silence mutant SPTLC1 (p.S331F) in a disease mouse model carrying heterozygous p.S331F mutation (S331F mice).

Gapmer ASOs, targeting the S331F variant in either 2'-O-Methyl (2'-OMe), locked nucleic acid (LNA) or 2'-O-methoxy ethyl (MOE) chemistries, were firstly studied in cultured mouse skin fibroblasts. The candidate ASOs in LNA or MOE were further evaluated *in vivo*.

Single subcutaneous injection of ASOs in neonatal or adult S331F mice achieved over 90% mutant transcripts silencing in the liver and dorsal root ganglia (DRG). Weekly subcutaneous injections of LNA-ASOs of either unconjugated or conjugated with N-acetylgalactosamine (GalNAc) in S331F mice showed that GalNAc-LNA-ASO presented higher efficiency than the unconjugated LNA-ASO in reducing the mutant transcripts in the liver, DRG and sciatic nerve, without affecting the wild-type transcripts. GalNAc-LNA-ASO also achieved significant

© The Author(s) 2025. Published by Oxford University Press on behalf of The Guarantors of Brain. This is an Open Access article distributed under the terms of the Creative Commons Attribution License (https://creativecommons.org/licenses/by/4.0/), which permits unrestricted reuse, distribution, and reproduction in any medium, provided the original work is properly cited.

ACCEPTED MANUSCRIPT

Downloaded from https://academic.oup.com/brain/advance-article/doi/10.1093/brain/awaf403/8297247 by DO NOT USE Institute of Education merged with 90002272 user on 29 October 2025

reduction in the blood levels of the neurotoxic metabolites 1-deoxysphingoidbases (1-deoxySL), a biomarker used in HSN1A patients.

Transcriptomic studies in DRGs demonstrated the involvement of the mitochondrial pathway in pathological changes of the S331F mice. Quantitative RT-PCR analysis confirmed the differentially expressed genes between the S331F and wildtype mice. Furthermore, these aberrantly expressed genes in S331F mice were reversed by the GalNAc-LNA-ASO treatment. Our data provides necessary *in vivo* evidence as proof-of-concept for ASO-mediated mutant allele-specific silencing as a therapeutic approach for SPTLC1-related HSN1.

Author affiliations:

1 Genetics and Genom ic Medicine Department, Great Ormond Street Institute of Child Health, University College London, WC1N 1EH, UK

2 NIHR Great Ormond Street Hospital Biomedical Research Centre, WC1N 1EH, UK

3 Institute for Clinical Chemistry, University Hospital and University of Zürich, 8006, Zürich, Switzerland

4 The Dubowitz Neuromuscular Centre, Developmental Neurosciences Department, Great Ormond Street Institute of Child Health, University College London, WC1N 1EH, UK

5 Department of Neuroscience, Physiology and Pharmacology, University College London, WC1E 6BT, UK

6 Centre of Neuroscience, Surgery and Trauma, Blizard Institute, Barts and the London School of Medicine and Dentistry, London, E1 2AT, UK

7 Neural Injury Group, Nuffield Department of Clinical Neuroscience, John Radcliffe Hospital, University of Oxford, OX3 9DU, UK

8 Neurodegenerative Disease Department, UCL Queen Square Institute of Neurology, London WC1N 3BG, UK

9 Department of Neuromuscular Diseases, UCL Queen Square Institute of Neurology, WC1N 3BG, UK

ACCEPTED MANUSCRIPT

Downloaded from https://academic.oup.com/brain/advance-article/doi/10.1093/brain/awaf403/8297247 by DO NOT USE Institute of Education merged with 90002272 user on 29 October 2025

Correspondence to: Haiyan Zhou, MD PhD

Genetics and Genomic Medicine Department, Great Ormond Street Institute of Child Health, University College London, London, WC1N 1EH, UK

E-mail: Haiyan.zhou@ucl.ac.uk

Running title: ASO therapy for SPTLC1-related neuropathy

Keywords: neurodegenerative disorder; antisense oligonucleotide (ASO); allele specific silencing; peripheral neuropathy; mouse model; biodistribution

Introduction

Hereditary sensory neuropathy type I (HSN1) is a neurodegenerative disorder, affecting 1 in 500, 000 individuals in the general population.[1] It is characterized by prominent sensory loss, neuropathic pain, and various degrees of limb weakness in advanced cases.[2] Loss of sensation can lead to painless injuries, resulting in slow wound healing, osteomyelitis and subsequent distal amputations. HSN1A is caused by mutations in the *Serine Palmitoyl Transferase Long Chain base subunit 1* (*SPTLC1*) gene, which encodes a subunit of serine palmitoyl transferase (SPT).[3] SPT catalyses the initial step in sphingolipid biosynthesis by conjugating palmitoyl-CoA with L-serine. Mutations in *SPTLC1* cause a shift in the substrate specificity of SPT, from serine to alanine and glycine, leading to the production of 1-deoxy-sphingolipids (1-deoxySL) (Fig.1A), which are toxic to neurons.[5-7] As 1-deoxySLs are produced by a gain-of-function, secondary to missense mutations in *SPTLC1* gene, and the fact that haploinsufficiency of SPTLC1 is not pathogenic,[4, 5, 8] selective silencing of the mutant transcripts while retaining the wild-type (WT) allele, may eliminate 1-deoxySL formation. Such an approach is particularly relevant given that, SPTLC1 is essential for the synthesis of canonical sphingolipids which have key roles in cell adhesion, inter-cellular signalling, and membrane dynamics, as homozygous loss-of-function in *Sptlc1* are embryonically lethal in mice.[8,9]

RNA-targeted therapy using antisense oligonucleotides (ASOs) offer great potential for neurodegenerative disorders. Gene-silencing ASOs have been successfully used in treating

ACCEPTED MANUSCRIPT

Downloaded from https://academic.oup.com/brain/advance-article/doi/10.1093/brain/awaf403/8297247 by DO NOT USE Institute of Education merged with 90002272 user on 29 October 2025

conditions caused by gain-of-function mutations, such as innotersen for TTR-related amyloidosis,[10] volanesorsen for familial chylomicronaemia syndrome,[11] and tofersen for amyotrophic lateral sclerosis (ALS).[12] While general downregulation of a protein, especially an enzyme, could be detrimental, a specific lowering of the mutant protein would be of benefit in some conditions. Selective mutant-allele downregulation is developed in Huntington's disease as an alternate to improve the previous clinical trials on a general gene silencing approach.[13] Allele-specific silencing ASOs have also been investigated in other dominant gain-of-function conditions, such as COL6-related muscular dystrophy.[14, 15] A small interfering RNA (siRNA) approach was tested in fibroblasts cultured from patients with childhood ALS caused by dominant *SPTLC1* mutations, a severe allelic condition to HSN1A, which silenced mutant transcripts and normalized the elevated levels of canonical SPT.[16]

Here, we investigate allele-specific ASO approach in an existing Sptlc1 mouse model, the S331F mice, which harbours a heterozygous S331F mutation in mouse *Sptlc1* gene. We describe the *in vivo* proof-of-concept studies on developing ASOs to target the S331F mutation in mice. ASOs in 2'-O-methyl (2'-OMe), 2'-O-methyloxyethyl (2'-MOE) and locked nucleic acids (LNA) were tested in mouse skin fibroblasts. The lead ASOs in LNA or MOE, as well as LNA conjugated with N-acetylgalactosamine (GalNAc) were further evaluated in S331F mice. Our data shows a specific suppression of the mutant *Sptlc1* mRNA *in vivo*, without affecting the WT *Sptlc1* transcripts. Repeated systemic ASOs treatment significantly reduced1-deoxySL in blood, confirming plasma levels of 1-deoxySL as a sensitive therapeutic biomarker. We also identify the involvement of mitochondrial pathways in S331F mice by next generation mRNA sequencing which appear to be modulated by effective ASO treatment. Our results demonstrate the feasibility of allele-specific ASO approach in treating SPTLC1-related HSN1 (SPTLC1-HSN1).

ACCEPTED MANUSCRIPT

Downloaded from https://academic.oup.com/brain/advance-article/doi/10.1093/brain/awaf403/8297247 by DO NOT USE Institute of Education merged with 90002272 user on 29 October 2025

Materials and methods

Study design

Studies were designed to investigate ASOs in silencing the mutant transcripts in the S331F mice and its effect on plasma levels of 1-deoxySL and transcriptomics in dorsal root ganglia (DRG) and liver. ASOs designed in different chemical modifications were tested in skin fibroblasts derived from S331F mice. The specific silencing effect on S331F transcripts was measured by allele-specific real-time PCR (qRT-PCR). The lead ASOs in MOE or LNA chemistries were then tested in S331F mice, either neonate or young adult, for a single subcutaneous injection and measured by qRT-PCR in liver, DRGs and sciatic nerves (SNs) at 7 days post-injection. The lead ASOs in MOE, LNA and GalNAc-conjugated LNA were further studied in adult S331F mice treated by weekly subcutaneous injections for 8 weeks, followed by qRT-PCR on mRNA expression in liver, DRGs and SNs, mass spectrometry measurement on plasma 1-deoxySL levels, and transcriptomic studies using next-generation mRNA sequencing in DRGs. Age-matched saline-treated S331F mice were used as controls. The number of mice required in each experiment was determined according to pilot studies and justified according to 3Rs principle. All experimental and control mice were allocated randomly, and all studies were conducted in a double-blinded manner.

ASOs

ASOs for *in vitro* studies were synthesized by Eurogentec Ltd. ASOs for *in vivo* studies were synthesized by Microsynth Ltd. GalNAc-conjugated ASOs were synthesized by AxoLabs GmbH.

Mouse procedures

The S331F mice (C57BL/6NTac-Sptlc1^{em1H}/H, stock code: SPTLC1-S331F-EM1-B6N) were obtained from the Mary Lyon Centre at MRC Harwell.[17] Mice heterozygous for S331F mutation (*S331F*$^{+/-}$) were crossed with WT C57BL/6N mice. Subcutaneous injections, blood and tissue collection were carried out in the Biological Services Unit University College London, in

ACCEPTED MANUSCRIPT

Downloaded from https://academic.oup.com/brain/advance-article/doi/10.1093/brain/awaf403/8297247 by DO NOT USE Institute of Education merged with 9000272 user on 29 October 2025

accordance with the Animals (Scientific Procedures) Act 1986. Experiments were performed under Home Office licence number PP2611161.

Mouse fibroblasts culture and ASO treatment

Skin fibroblasts were cultured from S331F mice. For lipofectamine 2000 transfection, cells were seeded into 24-well plates at a density of 5×10^4 cells/well, giving 80% confluence on the next day. ASOs were complexed with Lipofectamine 2000 (ThermoFisher) in Opti-MEM according to the manufacturer's instructions and incubated with cells for 24 hours before RNA extraction. For gymnotic treatment, fibroblasts were seeded at a density of 2×10^4 cells/well. The next day, ASOs were added to growth medium and cultured for 6 days before RNA extraction.

Allele-specific quantitative real-time reverse transcription PCR

Total RNA from cultured cells or mouse tissues were extracted using the Qiagen RNeasy Mini kit. Quantification of WT or S331F *Sptlc1* mRNA was performed using iTaq Universal One-Step RT-qPCR Kit (Bio-Rad, Watford, UK), with mouse *Hprt* the housekeeping gene. Primer sequences were provided in Supplementary Table 1.

SplintR PCR

Concentrations of ASOs in mouse tissues were measured by SplintR PCR according to protocol described previously.[18] Mouse tissues were lysed in RIPA buffer. The supernatant of tissue lysate was hybridized and ligated with probes using SplintR ligase kit (New England Biolabs, M0375S), following manufacture's instruction. After ligation, qRT-PCR was performed by PrimeTime™ Gene Expression Master Mix kit (integrated DNA technologies, 1055772) using primers and probes specifically designed to recognize the target ASOs (MOE-ASO1 and LNA-ASO1). The sequences of probes and primers were provided in supplementary data (Supplementary Table 5).

Mass spectrometry analysis

The plasma levels of 1-deoxySL were measured by multiple reaction monitoring- based liquid chromatography-mass spectrometry (LC-MRM-MS) method as previously described.[19] Briefly,

ACCEPTED MANUSCRIPT

Downloaded from https://academic.oup.com/brain/advance-article/doi/10.1093/brain/awaf403/8297247 by DO NOT USE Institute of Education merged with 9000272 user on 29 October 2025

lipid was extracted from 50µl plasma sample by adding 50µl of deionized water followed by 500µl of the lipid extraction solvent (100% methanol containing D7-C18SO and D7-C18SA, 200 pmol per sample). A chemical hydrolysis step was added to the extracted lipids prior to analysis. Long chain bases of sphingolipids extracted from lipid hydrolysates were quantified by MS using D7-C18SO and D7-C18SA as the internal standards. Mass spectra were subsequently collected in MRM positive ion mode. 1-deoxySO and 1-deoxySA were detected from the single dehydration product generated in the ion source using the declustering potential of 160 V. The sum of 1-deoxySO and 1-deoxySA concentrations was quantified as the level of 1-deoxySL.

Transcriptomics and RNA-Seq analysis

DRGs from all spinal levels were dissected from 3-months old male WT and S331F mice. Total RNA was extracted and quality controlled using Agilent Bioanalyser 2100 TapeStation System (UCL Genomics). Next-generation RNA sequencing was performed by Novogene (UK). FPKM (the expected number of Fragments Per Kilobase of transcript sequence per Millions base pairs sequenced), representing the abundance of transcripts (count of sequencing) that mapped to genome or exon, was used to estimate the level of gene expression. For high-confidence expression, FPKM ≥ 10 was used to filter out low-abundance transcripts. Non-coding mouse transcripts were excluded from the subsequent gene analysis. Differentially expressed genes (DEGs), analyzed by DESeq2 method, were determined when the event had sufficient read coverage (coverage ≥ 20), log2(FoldChange) ≥0, $p \leq 0.01$ and false discovery rate (FDR) ≤ 0.05. Enrichment studies were performed by Gene Ontology (GO) Enrichment, Kyoto Encyclopedia of Genes and Genomes (KEGG) and Reactome database Enrichment analysis on biological functions or pathways significantly associated with DEGs. GO terms, KEGG pathways and Reactome pathway enrichment with adjusted *p* value (*padj*) < 0.05 are deemed as significant enrichment.

Statistics

Comparisons between two groups were performed using unpaired Student's *t*-test (normal data) or Mann-Whitney U test (non-normal data), as appropriate. For comparison of three or more groups, one-way ANOVA followed by Tukey's test was used for normal data, or Kruskal-Wallis

ACCEPTED MANUSCRIPT

Downloaded from https://academic.oup.com/brain/advance-article/doi/10.1093/brain/awaf403/8297247 by DO NOT USE Institute of Education merged with 9000272 user on 29 October 2025

test followed by Dunn's tests for non-normal data. Data were analysed using two-way ANOVA and Sidak's multiple comparisons test for comparisons involving more than two groups across two independent factors (e.g. factors: [WT *vs*. Mut transcripts] × [saline *vs*. ASOs treatment]). Assumptions were verified via normality tests. Significance was set at $p < 0.05$. Results presented in this study are displayed as Mean ± Standard Error of the Mean (SEM). GraphPad Prism 10.0 software was used for statistical analysis and graph design. **p*<0.05, ***p*<0.01, ****p*<0.001 and *****p*<0.0001.

Results

ASOs selectively silence the mutant transcripts in skin fibroblasts cultured from the S331F mice

The S331F mice carry two heterozygous variants, c.990 C>G (a synonymous base change created during CRISPR/Cas9 genome editing when generating the c.992 C>T mutation) and c.992 C>T (the missense S331F variant) *in cis* in exon 11 of mouse *Sptlc1* gene (Fig. 1B). Nine gapmer ASOs were designed in either 2'-OMe, MOE or LNA chemical modifications. The two nucleotides complementary to c.990G and c.992T were placed in the central phosphorothioate-DNA sequence (Table 1).

Skin fibroblasts cultured from S331F mice were treated with ASOs at 10 nM for 24 hours with lipofectamine 2000, as the first round of ASOs screening. The mutant and WT transcripts were measured by allele-specific qRT-PCR (Primers are listed in Supplementary Table 1). All nine ASOs exhibited significant effects in distinguishing mutant transcripts from WT transcripts, by presenting more preferential silencing effect on mutant transcripts than WT transcripts (Fig. 2A). We next performed gymnosis studies on MOE and LNA-ASOs, considering their potential and satisfactory safety profile in clinical application. Fibroblasts were treated with ASOs at 10 μM for 6 days, in absence of transfection reagent. Except LNA-ASO3 which downregulated both WT and mutant transcripts, all the other ASOs showed efficient and preferential silencing on the mutant transcripts (Fig. 2B)

ACCEPTED MANUSCRIPT

Downloaded from https://academic.oup.com/brain/advance-article/doi/10.1093/brain/awaf403/8297247 by DO NOT USE Institute of Education merged with 9000272 user on 29 October 2025

We next conducted dose-response studies on MOE and LNA-ASOs (Fig. 2C and D). Mouse fibroblasts were treated with ASOs at a series of concentrations ranging from 0 to 50 nM under transfection of lipofectamine 2000 (Fig. 2C). Median inhibition concentration (IC50) values of ASOs on either mutant (IC50 Mut) or WT (IC50 WT) transcripts were used as parameters to indicate the silencing efficiency and specificity. The ratio of IC50 WT to IC50 Mut was also used to identify the lead compounds showing the highest specificity (Supplementary Table 1). The higher IC50 WT/Mut the more specific is the ASO for mutant over WT transcripts. LNA-ASO1 was determined to be the most potent candidate with IC50 Mut = 0.08 nM, IC50 WT = 3.00 nM and IC50 WT/Mut=37.5. MOE-ASO1, which shares the same nucleotides sequence as LNA-ASO1, also showed superior specificity in silencing mutant transcripts with IC50 Mut = 0.67 nM, IC50 WT = 13.56 nM and IC50 WT/Mut=20.24. LNA-ASO3 and MOE-ASO3 were also efficient in silencing mutant transcripts, however, with low specificity by silencing WT transcripts at the same time (Fig. 2C, Supplementary Table 2).

This was followed by dose-response gymnosis studies with ASOs at a concentration range of 0 to 10 μM (Fig. 2D). MOE-ASO1 showed the lowest IC50 Mut = 0.81 μM, followed by LNA-ASO3 with IC50 Mut = 0.99 μM. However, LNA-ASO3 also exhibited a strong silencing effect on WT allele (IC50 WT= 6.63 nM), suggesting a low discrimination between the two alleles (Fig. 2D, Supplementary Table 2).

Based on data from both lipofectamine transfection and gymnosis studies, we selected LNA-ASO1, LNA-ASO3 and MOE-ASO1 for further *in vivo* validation in S331F mice.

LNA-ASO1 selectively silence the mutant transcripts in S331F mice

Considering the significant silencing effect of the LNA-ASOs observed *in vitro*, our initial *in vivo* studies were focused on LNA-ASO1 and LNA-ASO3. To determine the lead ASO, we started with single dose studies in neonatal and adult mice.

Newborn S331F mice at postnatal day 3 (PND3) received a single subcutaneous injection of LNA-ASO1 or LNA-ASO3 at 25μg/g. Liver and dorsal root ganglia (DRGs) were collected at 7 days after the injection for the subsequent allele-specific qRT-PCR analysis. In mice treated with LNA-ASO1, a specific suppression of mutant allele was detected at 58% reduction in both the liver and DRGs, compared to saline treated age-matched S331F mice as control. There was no

ACCEPTED MANUSCRIPT

Downloaded from https://academic.oup.com/brain/advance-article/doi/10.1093/brain/awaf403/8297247 by DO NOT USE Institute of Education merged with 90002272 user on 29 October 2025

significant silencing on WT transcripts in either the liver or the DRGs (Fig. 3A). However, in mice treated with LNA-ASO3, mutant allele-specific silencing was only detected in the DRGs, with 88% reduction on mutant transcripts while no effect on WT transcripts. Significant reductions on both mutant and WT transcripts were detected in the liver, at 90% and 96%, respectively (Fig. 3A).

The distinct allele-specific silencing effect of LNA-ASO1 was also confirmed in 6-week-old adult S331F mice. A single subcutaneous injection of LNA-ASO1 at 25µg/g significantly reduced mutant transcripts by 94% in the liver and 70% in the DRGs (Fig. 3B). No silencing effect was detected on WT transcripts either in the liver or in the DRGs. In contrast, LNA-ASO3 showed no significant silencing effect on mutant transcripts (18%) in the liver, but a significant silencing effect on WT transcript (74%). In the DRGs, 96% mutant allele-specific silencing was detected when compared to saline-treated controls (Fig. 3B). The data from the single dose studies suggest LNA-ASO1 the lead ASO in achieving the desirable mutant-allele specific silencing in both neonatal and adult mice. LNA-ASO1 was selected as the lead compound for the subsequent *in vivo* studies.

Next, we assessed the duration of the silencing effect following a single subcutaneous injection. Six-week-old adult S331F mice were injected with LNA-ASO1 at 25 µg/g. The liver and DRGs were harvested at 14 days post-injection followed by allele-specific qRT-PCR analysis. The result showed that while there was still around 80% mutant allele silencing in the liver, no silencing effect on the DRGs was detectable anymore at 2 weeks after a single injection (Fig. 3C). This data suggests that repeated administration of LNA-ASO1 on a weekly basis may be necessary to achieve a long-term sustainable therapeutic effect.

To determine the optimal dose of LNA-ASO1 for the future repeated treatment, we conducted a dose-response study at 10, 15, 20 and 25 µg/g, and measured the allele-specific silencing effect by qRT-PCR in the liver and DRG at 7 days after a single injection. In the liver, significant mutant allele silencing was detected at all four doses, with striking effect at 15µg/g dose with 83% silencing. In the DRGs, mutant transcripts remained unaffected at 10µg/g dose. The silencing became evident from 15µg/g dose, at 39% silencing (Fig. 3D). No effect was detected on WT allele in neither liver nor DRG. Our result presents a clear dose-dependent manner of

ACCEPTED MANUSCRIPT

Downloaded from https://academic.oup.com/brain/advance-article/doi/10.1093/brain/awaf403/8297247 by DO NOT USE Institute of Education merged with 9000272 user on 29 October 2025

LNA-ASOs on mutant-allele specific silencing *in vivo*. 15μg/g was decided to be used in the following repeated treatment of LNA-ASO1.

GalNAc conjugated LNA-ASO1 exert improved allele-specific silencing in S331F mice

The liver is a central organ in lipid metabolism, including the biosynthesis of sphingolipids. To increase the bio-engagement of ASOs in hepatocytes, we conjugated LNA-ASO1 with GalNAc, the ligand to the asialoglycoprotein receptor (ASGPR), which is highly expressed in hepatocytes. Conjugation of ASOs to GalNAc can enhance their hepatocyte uptake by 20-30-fold.[20]

Considering in most patients with SPTLC1-associated HSN1 first symptoms appear between the second and third decade of life, we decided to conduct the repeated injection experiment in young adult mice. Four-week-old S331F mice were treated with weekly subcutaneous injection of either LNA-ASO1 at 15μg/g, or GalNAc-LNA-ASO1 at 4μg/g, for a total of eight injections (Fig. 4A). One week after the last injection, liver, DRGs and sciatic nerves were harvested for allele-specific qRT-PCR analysis.

In the liver, a significant downregulation of mutant transcripts was detected in both LNA-ASO1 and its GalNAc conjugates, at 90% ($p < 0.0001$) and 88% ($p < 0.0001$), respectively (Fig. 4B). In the DRGs, 31% downregulation of mutant transcripts was detected in LNA-ASO1 treated mice ($p = 0.0023$), compared to 67% downregulation in the GalNAc-LNA-ASO1 treated mice ($p < 0.0001$) (Fig. 4B). A significant difference was detected between the LNA-ASO1 and GalNAc-LNA-ASO1 groups ($p = 0.0005$). In sciatic nerves, 24% mutant transcripts downregulation was detected in LNA-ASO1 treated mice, which was further improved to 32% downregulation in GalNAc-LNA-ASO1 treated mice ($p = 0.0252$). No significant effects on WT transcripts were detected in liver, DRGs or sciatic nerves from LNA-ASO1 or GalNAc-LNA-ASO1 treated mice (Fig. 4B).

ACCEPTED MANUSCRIPT

Downloaded from https://academic.oup.com/brain/advance-article/doi/10.1093/brain/awaf403/8297247 by DO NOT USE Institute of Education merged with 9000272 user on 29 October 2025

Repeated MOE-ASO treatment specifically downregulated the mutant transcripts in S331F mice

Our *in vitro* studies indicated MOE-ASO1 as the second most efficient ASO after LNA-ASO1 in specifically silencing mutant transcripts (Fig. 2C). However, in the following *in vivo* studies in either new-born or adult S331F mice, a single subcutaneous injection of MOE-ASO1 at 50µg/g did not show any silencing effects on mutant transcripts (Supplementary Fig. 1). Nevertheless, considering the wide and promising application of MOE chemistry in ASO clinical translations, we decided to continue the studies of repeated MOE-ASO1 treatment on its long-term efficacy in mice. Four-week-old S331F mice received weekly subcutaneous injection of MOE-ASO1 at 50µg/g for 8 weeks. One week after the last injection, the liver, DRGs and sciatic nerves were harvested for allele-specific qRT-PCR analysis. Significant mutant-allele specific silencing was detected in all three organs, with 84% downregulation in the liver ($p = 0.001$), 39% in the DRGs ($p = 0.0007$) and 39% in the sciatic nerves ($p = 0.02$) (Fig. 4C). No silencing effects on WT transcripts were detected in any of the organs.

ASOs reached high tissue concentrations in a wide range of peripheral organs after 8 weeks treatment

SPTLC1 is ubiquitously expressed, and sphingolipid biosynthesis is essential in all organs. To understand the *in vivo* biodistribution of LNA-ASO1 and MOE-ASO1, we have performed SplintR PCR analysis to examine tissue concentration.[18] In addition to the liver, DRGs and sciatic nerve, other organs such as kidney, heart, lung, spleen, skeletal muscle and skin were also collected for SplintR analysis, from the S331F mice received repeated ASO treatment. While no tissue concentration was detected in saline control mice, a body-wide bio-distribution of ASOs was detected in ASO-treated groups (Fig. 4D) (Supplementary Table 3). In LNA-ASO1 treated mice, kidneys presented the highest concentration of ASOs at 167.03×10^4 pM, followed by 24.64×10^4 pM in the liver. Further assessment on plasma levels of blood urea nitrogen (BUN) excluded potential kidney toxicity in any of the treatment groups (Supplementary Fig. 2). The heart, skin, skeletal muscle and DRG present similar tissue concentrations in a range between 10^4 to 10^5 pM, and low concentration in the lung and spleen at 10^3 pM. In MOE-ASO1 treated mice,

ACCEPTED MANUSCRIPT

Downloaded from https://academic.oup.com/brain/advance-article/doi/10.1093/brain/awaf403/8297247 by DO NOT USE Institute of Education merged with 9000272 user on 29 October 2025

high tissue concentrations were detected in a wide range of peripheral organs after 8 weeks treatment, with Liver (5.3×10^6 pM), skin (5.1×10^6 pM) and sciatic nerves (4.9×10^6 pM) presenting the highest tissue concentrations (Fig. 4D, Supplementary Table 3). Our study suggests that repeated subcutaneous injections of LNA-ASO at 15 µg/g or MOE-ASO at 50 µg/g are efficient in delivering ASOs in a wide range of peripheral organs.

Effective ASO treatment reduced the blood levels of 1-deoxySL in S331F mice

Increased plasma levels of 1-deoxySL, the sum of 1-deoxySO and 1-deoxySA, is a hallmark and biochemical biomarker correlated with clinical measures for HSN1A.[5, 21] To understand the sphingolipid profile and how it changes with disease progression in the S331F mice, we conducted a detailed mass spectrometry study on sphingolipids profiling in blood samples collected from mice at different ages, including PND 7, 14, 28, 49 and 56 days. A distinct sphingolipid signature was detected in the S331F mice compared to age-matched WT controls. The highest levels of 1-deoxySL were detected in the S331F mice at PND7 which then decreased with age (Fig. 5A). At each timepoints, the plasma levels of 1-deoxySL were consistently and significantly increased in the S331F mice compared to the age-matched WT controls (Fig. 5A). Further studies on gender difference in the plasma levels of 1-deoxySL in 28-day-old and 56-day-old WT and S331F mice, showed no difference between the male and female mice in any of the groups (Supplementary Fig. 3).

We continued to measure the plasma levels of 1-deoxySL in response to ASO treatment. Blood samples were collected from S331F mice that received a single or repeated ASO treatment as described above. In the single dose group, there were significant reductions in 1-deoxySL from LNA-ASO1 ($p = 0.021$) and LNA-ASO3 treated neonatal mice ($p = 0.025$) compared to saline-treated S331F mice (Fig. 5B). In adult mice, MOE-ASO1 showed a significant reduction in 1-deoxySL after a single dose treatment ($p < 0.001$) (Fig. 5C).

To understand the effect of long-term ASO treatment on plasma levels of 1-deoxySL, we collected blood samples from adult S331F mice received weekly ASO treatment for either 4 weeks or 8 weeks of LNA-ASO1, GalNAc-LNA-ASO1 or MOE-ASO1 as described above. There was no reduction in 1-deoxySL in LNA-ASO1 treated S331F mice after 4 or 8 weeks of

ACCEPTED MANUSCRIPT

Downloaded from https://academic.oup.com/brain/advance-article/doi/10.1093/brain/awaf403/8297247 by DO NOT USE Institute of Education merged with 9000272 user on 29 October 2025

treatment (Fig. 5D, E). Interestingly, the effects were significantly improved by GalNAc conjugation. GalNAc-LNA-ASO1 significantly reduced 1-deoxySL levels after 4 or 8 weeks of treatment, compared to unconjugated LNA-ASO1 treated ($p = 0.01$ and $p = 0.002$, respectively) or saline-treated S331F mice ($p = 0.002$ and $p = 0.005$, respectively) (Fig. 5D, E). 8 weeks of GalNAc-LNA-ASO1 treatment also showed significant reduction in 1-deoxySL further to 4 weeks of treatment ($p = 0.02$) (Fig. 5F). These results suggest that plasma levels of 1-deoxySL can be used as a biochemical biomarker to indicate the therapeutic response, and GalNAc conjugation can improve the therapeutic effect of LNA-ASOs in reducing 1-deoxySL.

Transcriptomics studies in S331F mice and its response to ASO treatment

We next investigated the transcriptomics profile in S331F mice, to identify the underlying molecular pathways and relevant transcriptomics which may be used as potential molecular markers to indicate the response to efficacious ASO treatment. Next generation mRNA sequencing was performed in DRGs isolated from three-month-old male WT and S331F mice (N=3/group).

Principal component analysis (PCA) plot showed that all the WT samples were clustered while the S331F samples were scattered (Supplementary Fig. 4a). Sample correlation showed close correlations among all the tested samples (Supplementary Fig. 4b), suggesting no significant segmentation between WT and S331F samples, which is in line with the subtle phenotype variations between WT and the S331F mice at this age.

143 differentially expressed genes (DEGs) were identified between the S331F and WT mice, (Supplementary Fig. 3c, Supplementary Table 4). Gene Ontology (GO) enrichment analysis of the 143 DEGs identified 11 most significantly enriched pathways (Fig. 6A, left) Kyoto Encyclopaedia of Genes and Genomes (KEGG) enrichment analysis of the 143 DEGs identified 4 most significantly enriched pathways (Fig. 6A, middle), including Oxidative phosphorylation, Non-alcoholic fatty liver disease, Cardiac muscle contraction and Retrograde endocannabinoid signalling. Reactome database Enrichment analysis identified 9 enriched pathways (Fig. 6, right), including Nonsense-mediated decay (NMD), nonsense mediated decay enhanced by the exon junction complex, Respiratory electron transport, ATP synthesis by chemiosmotic coupling and

ACCEPTED MANUSCRIPT

Downloaded from https://academic.oup.com/brain/advance-article/doi/10.1093/brain/awaf403/8297247 by DO NOT USE Institute of Education merged with 90002272 user on 29 October 2025

heat production by uncoupling proteins, the citric acid cycle and respiratory electron transport, formation of ATP by chemiosmotic coupling and cristae formation. These were followed by Mitochondrial biogenesis, Complex I biogenesis and Respiratory electron transport.

From all the DEGs identified by the enrichment analysis, pathways associated with mitochondrial function were strongly indicated. We then selected four genes with the highest functional relevance and fold changes, including *Mt-co2*, *Gapdh*, *Mt-ATP6, and Slc38a5*, for further validation. Their differential expression in the liver and DRGs were assessed by qRT-PCR in more WT and S331F mice (Primers are listed in Supplementary Table 1). As the RNA-Seq data were derived from DRGs from male mice, to avoid any potential effect of sex difference, the subsequent validation was performed in both male and female mice (*n*=4 mice/sex/group) (Fig. 6B).

Increased expression of *Mt-Co2*, *Gapdh*, *Slc38a5* and *Mt-ATP6* mRNA expression in DRGs from both male and female mice were confirmed by qRT-PCR (Fig. 6B, top). No gender effect on these genes was detected in the DRGs. However, clear discrepancies were detected in the liver, where significantly decreased *Mt-co2*, *Gapdh*, *Slc38a5* and *Mt-ATP6* transcripts were detected in female S331F mice, but significantly increased *Gapdh* transcripts were detected in male S331F mice (Fig. 6B, bottom). Our data suggests a significant gender effect on these genes in the liver, and female S331F mice showed more significant changes in relevant transcriptomics in the liver.

Based on these data, we next investigated the response of these genes to repeated ASOs treatment in female S331F mice. qRT-PCRs of *Mt-co2*, *Gapdh*, *Slc38a5* and *Mt-ATP6* transcripts were performed in liver and DRGs from female WT (*n*=4), S331F (*n*=4), and S331F mice received 8 weeks of ASOs treatment, including LNA-ASO1(*n* = 5), GalNAc-LNA-ASO1 (*n* = 5) and MOE-ASO1 (*n*= 4).

In the DRGs, increased transcripts were detected in all four genes in female S331F, compared to WT mice. *Mt-Co2*, *Mt-ATP6* and *Gapdh* did not show any response to ASOs treatment (Fig. 6C). Interestingly, significant increase in *Scl38a5* transcripts was detected after the treatment of GalNAc-LNA-ASO1 or MOE-ASO1. In the liver, compared to saline-treated S331F mice, *Slc38a5*, *Gapdh* and *Mt-ATP6* showed significant response to GalNAc-LNA-ASO1 treatment which corrected their expression towards the WT levels (Fig. 6D). Mt-Co2 also showed a trend

ACCEPTED MANUSCRIPT

Downloaded from https://academic.oup.com/brain/advance-article/doi/10.1093/brain/awaf403/8297247 by DO NOT USE Institute of Education merged with 9000272 user on 29 October 2025

of increased expression after GalNAc-LNA-ASO1 treatment, although not statistically significant ($p = 0.054$). This result is consistent with the data above where GalNAc-LNA-ASO1 showed the highest therapeutic effect in the liver compared to its effect in the DRGs and to other unconjugated ASOs (Fig. 4 and Fig. 5).

Discussion

SPTLC1-HSN1 is a devastating and progressive neurodegenerative peripheral neuropathy with no disease modifying treatment currently available. Supplementation with L-serine competes with L-alanine and L-glycine for the binding site of SPT and has been shown to reduce the production of blood 1-deoxySL levels in the C133W-Sptlc1 mouse model and in patients carrying C133Y mutation.[21] A pilot clinical study of high doses L-serine (NCT01733407) suggest it may slow down the clinical progression of the disease[21], and a subsequent clinical trial is currently ongoing (NCT06113055). At present there is no other therapeutic intervention approved, and an effective therapy is desperately needed. In this study, we provide necessary *in vivo* evidence as proof-of-concept for the development of allele-specific ASO therapy for SPTLC1-HSN1.

In SPTLC1-HSN1, the primary and most prominent feature is peripheral sensory defects universally present in all patients, although motor defects are also detected in some patients, especially in men. Therefore, in this pilot study we only concentrate on testing the ASO approach in targeting peripheral organs. In this study, the ASOs in MOE or LNA chemical modifications showed an efficient biodistribution and target engagement in the disease-related peripheral organs, including the liver, DRGs and sciatic nerves. Moreover, significantly enhanced efficacy was achieved from GalNAc-conjugated LNA-ASO at both mRNA and biochemistry levels (Figs 4 and 5). GalNAc-ASO conjugates are used to enhance ASO uptake in hepatocytes.[22, 23] Several FDA-approved RNA drugs use this approach, for example, eplontersen, an ASO conjugated to GalNAc, and vutrisiran, an siRNA conjugated to GalNAc, are used for the treatment of hereditary transthyretin amyloidosis, which have dramatically improved the clinical efficacy and safety profile, compared to the original unconjugated counterparts. [24,25] The synergistic effect between LNA-ASO and GalNAc conjugation in this study not only suggests

ACCEPTED MANUSCRIPT

Downloaded from https://academic.oup.com/brain/advance-article/doi/10.1093/brain/awaf403/8297247 by DO NOT USE Institute of Education merged with 9000272 user on 29 October 2025

the liver as one of the key target organs in HSN1, in addition to sensory neurons and peripheral nerves, but also indicates the importance of the conjugation method in enhancing the *in vivo* efficacy of ASOs. While unconjugated gapmer ASOs have demonstrated clinical success with notable examples from *inotersen, volanesorsen*, and *tofersen*, we remain cautious about the potential dose-dependent toxicity associated with gapmer ASO, as evidenced by some setback in clinical trials, such as the ASO trials for centronuclear myopathy[26] and Huntington's Disease.[27] Therefore, future studies are needed to investigate more formulated ASOs with different conjugates, such as fatty acids or transferrin receptor-binding molecules,[28, 29, 30] beyond GalNAc, to enhance ASO targeting not only in peripheral organs but also in motor neurons within the central nervous system, maximizing the therapeutic potential of the ASO approach.

The ASOs were in gapmer design to specifically target the transcripts carrying the S331F mutation in mouse *Sptlc1* gene and exerted allele-specific mRNA silencing via RNase H cleavage. It is noted that the heterozygous S331F mice carry two heterozygous nucleotide mismatches, the synonymous c.990 C>G variant (which was inserted in order to generate the mutant mouse by CRISPR/Cas9 technology as it prevents re-cutting of the allele) and the c.992 C>T (p.S331F) missense variant. The former silent variant is not predicted to impact on functional effects of the allele. However, this does make the allele discrimination more efficient than those with a single nucleotide change which represents the majority of dominant toxic gain-of-function conditions. We have recently reported several strategies to improve the design of allele-specific silencing, including the design of multimers based on predicted secondary structure of target sequence, and the introduction of additional nucleotide mismatches to increase the silencing specificity.[14] In the real world, mutation-specific ASO approach presents limited clinical application in conditions where most cases are sporadic. Therefore, ASOs designed to target common mutations or common single nucleotide polymorphism (SNP) were developed for alleles discrimination. In SPTLC1-HSN1, the p.C133W (c.399T>G) missense mutation represents the most common pathogenic variant as a founder mutation in cohorts of patients from the UK, Australia, Canada and USA.[1, 3, 31] Supported by the present proof-of-concept studies, allele-specific ASOs by targeting the founder heterozygous C133W mutation represents a promising experimental ASO therapy for the largest cohort of SPTLC1-HSN1 patients, a project currently under development. In addition to HSN1, successful development of the allele-specific ASO approach may also benefit patients affected by SPTLC1-associated childhood ALS. In

ACCEPTED MANUSCRIPT

Downloaded from https://academic.oup.com/brain/advance-article/doi/10.1093/brain/awaf403/8297247 by DO NOT USE Institute of Education merged with 9000272 user on 29 October 2025

contrast to SPTLC1-HSN1 where HSN1-causing variants increase alanine usage by SPT leading to the formation of deoxy-sphingolipids, ALS-causing variants result in increased production of sphinganine and ceramides. [16] In addition, SPTLC1-related juvenile ALS patients present early-childhood-onset and exclusive motor involvement, including loss of ambulation and respiratory insufficiency, without any sign of sensory involvement. [16] This suggests that allele-specific gene silencing approach can be used in both conditions, with SPTLC1-HSN1 primarily on targeting peripheral neuropathy whilst SPTLC1-ALS more on motor neurons targeting.

HSN1 has a juvenile to adult onset. While the median age at first symptom onset in patients with HSN1 was 23 years, many patients reported sensory symptoms in early- to mid-teenage years.[32] In most patients, it is likely the harm from the accumulated neurotoxic 1-deoxySL begins in childhood. Indeed, in this study we confirmed the strikingly elevated blood 1-deoxySL levels in neonatal S331F mice (Fig. 5A). Our results also indicate that neonatal mice may have a better response to ASOs than adult mice in abolishing the production of 1-deoxySL (Fig 5B). While in this study our repeated treatment only focused on young adult mice from 4 weeks old, it is reasonable to assume that early treatment at the presymptomatic stage, such as in children or young teens, may provide more benefit than treatment in adults. To achieve this, a validated clinical biomarker, for example the plasma levels of 1-deoxySL, will be needed to guide this therapeutic regimen. Benefited from the advanced genetic diagnosis, many patients carrying the C133W founder mutation in the UK receive the presymptomatic diagnoses. These patients are likely to benefit more from a presymptomatic ASO treatment if the hypothesis is confirmed.

The S331F mutation is associated with a severe and early on-set clinical phenotype in two sporadic patients with HSN1A.[33] In contrast, the S331F mice did not exhibit any prominent neurophysiological or pathological phenotype at the current study age, similar to the previously published mouse model of the C133W mutation where no distinct neuropathy phenotype detected until aged adulthood. [34] This has limited our studies on some relevant clinical outcomes in response of ASO treatment. Increased 1-deoxySL levels were detected in cultured HEK293T cells expressing the p.S331F-SPTLC1 constructs.[35] In HSN1 patients plasma levels of 1-deoxySL were reported to be elevated in all patients compared with healthy controls, and correlated moderately with CMTNSv2 (CMT neuropathy score version 2) in males.[32] Further evidence of plasma 1-deoxySL as a potential biomarker for HSN1 arise from a recent L-serine clinical trial (NCT01733407) where plasma levels of 1-deoxySL were correlated with CMTNS

ACCEPTED MANUSCRIPT

Downloaded from https://academic.oup.com/brain/advance-article/doi/10.1093/brain/awaf403/8297247 by DO NOT USE Institute of Education merged with 9000272 user on 29 October 2025

(CMT neuropathy score) and reduced after L-serine treatment (59% decrease in serine treated vs 11% increase in placebo; $p < 0.001$).[36] In our study, elevated plasma 1-deoxySL levels were detected in S331F mice, starting from neonates (Fig. 5A), and responded to efficient ASOs treatment. Therefore, from a drug development point of view the plasma levels of 1-deoxySL in young mice are likely a more efficient biomarker than other late clinical outcomes in aged mice, especially if the treatment needs to commence in early age.

Our transcriptomic studies further indicate mitochondrial dysfunction as a key pathway in the pathogenesis of SPTLC1-HSN1, as supported by the enriched pathways studies and the subsequent validation on the differential expression of *Slc38a5, Gapdh, Mt-Co2* and *Mt-ATP6* genes in the DRGs and liver in the S331F mice and their response to efficient ASO treatment (Fig.6). *Slc38a5* (Solute Carrier Family 38 Member 5) is a sodium-coupled neutral amino acid transporter, primarily involved in the transport of neutral amino acids including glutamine, alanine, and serine.[37] Deletion of Slc38a5 in mice leads to accumulation of 1-deoxySL, mitochondrial abnormalities and motor impairment.[38] Therefore, the significantly increased expression of *Slc38a5* in the DRGs and liver of S331F mice after ASOs treatment may be considered as a positive therapeutic response (Fig. 6C and D). *Gapdh* (Glyceraldehyde-3-Phosphate Dehydrogenase) is a key enzyme in glycolysis and involved in cell death and mitochondrial function.[39] *Mt-Co2*, or cytochrome c oxidase subunit II, is a crucial component of the cytochrome c oxidase complex (Complex IV) in the mitochondrial respiratory chain involved in the transfer of electrons from cytochrome c to oxygen. Mt-ATP6 encodes a subunit of ATP synthase (also known as complex V), a crucial enzyme in the final step of oxidative phosphorylation, which produces ATP, the cell's main energy source. Both *Mt-Co2* and *Mt-ATP6* are crucial to mitochondria function. Mitochondrial dysfunction is a hallmark of SPTLC1-HSN1. Mutations in the SPTLC1 protein cause mitochondrial structural abnormalities and endoplasmic reticulum (ER) stress in lymphoblasts.[40] Exogenous application of 1-deoxySL to cultured primary mouse neurons changes intracellular Ca^{2+} handling in ER and mitochondria and causes an early loss of mitochondrial membrane potential.[6] Further functional assessment on these pathways, such as seahorse assay on patient fibroblasts or iPSC-derived neurons,[7] may provide more information on molecular mechanisms and molecular markers for this condition. In addition, a gender difference in these mitochondria-related genes expression was noticed in the transcriptomic studies in S331F mice, especially in the liver. This is of particular interest as some

ACCEPTED MANUSCRIPT

Downloaded from https://academic.oup.com/brain/advance-article/doi/10.1093/brain/awaf403/8297247 by DO NOT USE Institute of Education merged with 9000272 user on 29 October 2025

males with C133W SPTLC1-HSN1 present earlier and with a more severe phenotype. Our study indicates that further investigation into gender differences in SPTLC1-HSN1, both in patient populations and mouse models, are needed. Gender-specific responses in neurobehavioral studies and treatment efficacy could significantly influence the interpretation of results in mouse models and the design of outcome measures for future ASO therapy trials.

In conclusion, out study shows the therapeutic effect of allele-specific ASOs in selectively silencing mutant transcripts in the S331F mouse model. Our data suggests that targeting the liver by GalNAc-conjugated ASOs is more efficient in reducing plasma 1-deoxySL levels with enhanced target engagement not only in the liver but also in the DRGs and peripheral nerves. Furthermore, we demonstrated the potential of plasma 1-deoxySLs as biochemical biomarkers to assess the therapeutic efficacy of ASO treatment in SPTLC-HSN1, and the need of early therapeutic intervention prior to symptom onset. The identification of mitochondrial pathway involvement provides further insights into the disease pathophysiology and potential molecular markers of STPLC-HSN1. Our study provides strong *in vivo* evidence for developing ASO therapy for patients with SPTLC1-HSN1, a rare disease with high unmet needs and no current therapeutic options.

Data availability

All data is available in the main text or the supplementary materials. Requests for the S331F mice should be made directly to the MRC Harwell Institute under a material transfer agreement.

Acknowledgements

The authors would like to thank the funding and project management support from the Harrington Discovery Institute and the Oxford-Harrington Rare Disease Centre. The Mary Lyon Centre at MRC Harwell (MLC) is acknowledged for distributing the S331F mouse colony on behalf of the European Mouse Mutant Archive (www.infrafrontier.eu, Repository number EM:14648). The MLC generated the C57BL/6NTac-Sptlc1^{em1H}/H mouse strain as part of its commitment to the Genome Editing Mice for Medicine project funded [MC_UP_1502/3] by the

ACCEPTED MANUSCRIPT

Downloaded from https://academic.oup.com/brain/advance-article/doi/10.1093/brain/awaf403/8297247 by DO NOT USE Institute of Education merged with 90002272 user on 29 October 2025

Medical Research Council. The research reported in this publication is solely the responsibility of the authors and does not necessarily represent the official views of the Medical Research Council. The authors would also like to thank the MRC Centre for the Neuromuscular Centre Biobank in the Dubowitz Neuromuscular Centre, Great Ormond Street Institute of Child Health, University College London for providing relevant cell lines for research.

Funding

This work was funded by Harrington UK Rare Disease Scholar Award, RTW Foundation, Rosetrees Trust (PGL24/100137) and UCL Therapeutic Accelerator Scheme to HZ, Medical Research Council (MR/Y008405/1 and MR/X008029/1) and National Institute of Health Research UK, Great Ormond Street Hospital Biomedical Research Centre to HZ and FM. The thumbnail image for the online table of conents was created in BioRender. Zhou, H. (2025) https://BioRender.com/b56l4sc.

Competing interests

HZ, FM and MMR share a patent on Allele-Specific Gene Suppression (PCT/GB2017/050624 - WO/2017/153753). No competing interest is claimed by the other authors.

Supplementary material

Supplementary material is available at *Brain* online.

References

1. Davidson G, Murphy S, Polke J, et al. Frequency of mutations in the genes associated with hereditary sensory and autonomic neuropathy in a UK cohort. J Neurol. 2012;259(8):1673-85.

ACCEPTED MANUSCRIPT

Downloaded from https://academic.oup.com/brain/advance-article/doi/10.1093/brain/awaf403/8297247 by DO NOT USE Institute of Education merged with 90002272 user on 29 October 2025

2. Houlden H, King R, Blake J, et al. Clinical, pathological and genetic characterization of hereditary sensory and autonomic neuropathy type 1 (HSAN I). Brain. 2006;129(Pt 2):411-25.

3. Bejaoui K, Wu C, Scheffler MD, et al. SPTLC1 is mutated in hereditary sensory neuropathy, type 1. Nat Genet. 2001;27(3):261-2.

4. Eichler FS, Hornemann T, McCampbell A, et al. Overexpression of the wild-type SPT1 subunit lowers desoxysphingolipid levels and rescues the phenotype of HSAN1. J Neurosci. 2009;29(46):14646-51.

5. Penno A, Reilly MM, Houlden H, et al. Hereditary sensory neuropathy type 1 is caused by the accumulation of two neurotoxic sphingolipids. J Biol Chem. 2010;285(15):11178-87.

6. Wilson ER, Kugathasan U, Abramov AY, et al. Hereditary sensory neuropathy type 1-associated deoxysphingolipids cause neurotoxicity, acute calcium handling abnormalities and mitochondrial dysfunction in vitro. Neurobiol Dis. 2018;117:1-14.

7. Clark AJ, Kugathasan U, Baskozos G, et al. An iPSC model of hereditary sensory neuropathy-1 reveals L-serine-responsive deficits in neuronal ganglioside composition and axoglial interactions. Cell Rep Med. 2021;2(7):100345.

8. Hojjati MR, Li Z, and Jiang XC. Serine palmitoyl-CoA transferase (SPT) deficiency and sphingolipid levels in mice. Biochim Biophys Acta. 2005;1737(1):44-51.

9. Hannun YA, and Obeid LM. Principles of bioactive lipid signalling: lessons from sphingolipids. Nat Rev Mol Cell Biol. 2008;9(2):139-50.

10. Benson MD, Waddington-Cruz M, Berk JL, et al. Inotersen Treatment for Patients with Hereditary Transthyretin Amyloidosis. N Engl J Med. 2018;379(1):22-31.

11. Witztum JL, Gaudet D, Freedman SD, et al. Volanesorsen and Triglyceride Levels in Familial Chylomicronemia Syndrome. N Engl J Med. 2019;381(6):531-42.

12. Miller TM, Cudkowicz ME, Genge A, et al. Trial of Antisense Oligonucleotide Tofersen for SOD1 ALS. N Engl J Med. 2022;387(12):1099-110.

ACCEPTED MANUSCRIPT

Downloaded from https://academic.oup.com/brain/advance-article/doi/10.1093/brain/awaf403/8297247 by DO NOT USE Institute of Education merged with 90002272 user on 29 October 2025

13. Carroll JB, Warby SC, Southwell AL, et al. Potent and selective antisense oligonucleotides targeting single-nucleotide polymorphisms in the Huntington disease gene / allele-specific silencing of mutant huntingtin. Mol Ther. 2011;19(12):2178-85.

14. Aguti S, Cheng S, Ala P, Briggs S, Muntoni F, and Zhou H. Strategies to improve the design of gapmer antisense oligonucleotide on allele-specific silencing. Mol Ther Nucleic Acids. 2024;35(3):102237.

15. Marrosu E, Ala P, Muntoni F, and Zhou H. Gapmer Antisense Oligonucleotides Suppress the Mutant Allele of COL6A3 and Restore Functional Protein in Ullrich Muscular Dystrophy. Mol Ther Nucleic Acids. 2017;8:416-27.

16. Mohassel P, Donkervoort S, Lone MA, et al. Childhood amyotrophic lateral sclerosis caused by excess sphingolipid synthesis. Nat Med. 2021;27(7):1197-204.

17. Codner GF, Mianné J, Caulder A, et al. Application of long single-stranded DNA donors in genome editing: generation and validation of mouse mutants. (1741-7007 (Electronic)).

18. Shin M, Meda Krishnamurthy P, Devi G, and Watts JK. Quantification of Antisense Oligonucleotides by Splint Ligation and Quantitative Polymerase Chain Reaction. Nucleic Acid Ther. 2022;32(1):66-73.

19. Hülsmeier AJ, Gunasegaram L, Wipfli F, Lone MA, and Hornemann T. Long Chain Base Profiling with Multiple Reaction Monitoring Mass Spectrometry. (1940-6029 (Electronic)).

20. Debacker AJ, Voutila J, Catley M, Blakey D, and Habib N. Delivery of Oligonucleotides to the Liver with GalNAc: From Research to Registered Therapeutic Drug. Mol Ther. 2020;28(8):1759-71.

21. Garofalo K, Penno A, Schmidt BP, et al. Oral L-serine supplementation reduces production of neurotoxic deoxysphingolipids in mice and humans with hereditary sensory autonomic neuropathy type 1. J Clin Invest. 2011;121(12):4735-4522.

22. Prakash TP, Graham MJ, Yu J, et al. Targeted delivery of antisense oligonucleotides to hepatocytes using triantennary N-acetyl galactosamine improves potency 10-fold in mice. Nucleic Acids Res. 2014;42(13):8796-807.

ACCEPTED MANUSCRIPT

Downloaded from https://academic.oup.com/brain/advance-article/doi/10.1093/brain/awaf403/8297247 by DO NOT USE Institute of Education merged with 90002272 user on 29 October 2025

23. Huang Y. Preclinical and Clinical Advances of GalNAc-Decorated Nucleic Acid Therapeutics. Mol Ther Nucleic Acids. 2017;6:116-32.

24. Adams D, Tournev IL, Taylor MS, et al. Efficacy and safety of vutrisiran for patients with hereditary transthyretin-mediated amyloidosis with polyneuropathy: a randomized clinical trial. Amyloid. 2023;30(1):1-9.

25. Coelho T, Marques W, Jr., Dasgupta NR, et al. Eplontersen for Hereditary Transthyretin Amyloidosis With Polyneuropathy. Jama. 2023;330(15):1448-58.

26. Stinissen L, Böhm J, Bouma S, et al. Lessons Learned From Clinical Studies in Centronuclear Myopathies: The Patient Perspective-A Qualitative Study. Clin Ther. 2024;46(10):742-51.

27. McColgan P, Thobhani A, Boak L, et al. Tominersen in Adults with Manifest Huntington's Disease. N Engl J Med. 2023;389(23):2203-5.

28. Kaburagi H, Nagata T, Enomoto M, et al. Systemic DNA/RNA heteroduplex oligonucleotide administration for regulating the gene expression of dorsal root ganglion and sciatic nerve. Mol Ther Nucleic Acids. 2022;28:910-9.

29. Prakash TP, Mullick AE, Lee RG, et al. Fatty acid conjugation enhances potency of antisense oligonucleotides in muscle. Nucleic Acids Res. 2019;47(12):6029-44.

30. Barker SJ, Thayer MB, Kim C, et al. Targeting the transferrin receptor to transport antisense oligonucleotides across the mammalian blood-brain barrier. Sci Transl Med. 2024;16(760):eadi2245.

31. Dawkins JL, Hulme DJ, Brahmbhatt SB, Auer-Grumbach M, and Nicholson GA. Mutations in SPTLC1, encoding serine palmitoyltransferase, long chain base subunit-1, cause hereditary sensory neuropathy type I. Nat Genet. 2001;27(3):309-12.

32. Kugathasan U, Evans MRB, Morrow JM, et al. Development of MRC Centre MRI calf muscle fat fraction protocol as a sensitive outcome measure in Hereditary Sensory Neuropathy Type 1. J Neurol Neurosurg Psychiatry. 2019;90(8):895-906.

ACCEPTED MANUSCRIPT

Downloaded from https://academic.oup.com/brain/advance-article/doi/10.1093/brain/awaf403/8297247 by DO NOT USE Institute of Education merged with 90002272 user on 29 October 2025

33. Suh BC, Hong YB, Nakhro K, Nam SH, Chung KW, and Choi BO. Early-onset severe hereditary sensory and autonomic neuropathy type 1 with S331F SPTLC1 mutation. Mol Med Rep. 2014;9(2):481-6.

34. McCampbell A, Truong D, Broom DC, et al. Mutant SPTLC1 dominantly inhibits serine palmitoyltransferase activity in vivo and confers an age-dependent neuropathy. Hum Mol Genet. 2005;14(22):3507-21.

35. Rotthier A, Penno A, Rautenstrauss B, et al. Characterization of two mutations in the SPTLC1 subunit of serine palmitoyltransferase associated with hereditary sensory and autonomic neuropathy type I. Hum Mutat. 2011;32(6):E2211-25.

36. Fridman V, Suriyanarayanan S, Novak P, et al. Randomized trial of l-serine in patients with hereditary sensory and autonomic neuropathy type 1. Neurology. 2019;92(4):e359-e370.

37. Hägglund MG, Sreedharan S, Nilsson VC, et al. Identification of SLC38A7 (SNAT7) protein as a glutamine transporter expressed in neurons. J Biol Chem. 2011;286(23):20500-11.

38. Radzishevsky I, Odeh M, Bodner O, et al. Impairment of serine transport across the blood-brain barrier by deletion of Slc38a5 causes developmental delay and motor dysfunction. Proc Natl Acad Sci U S A. 2023;120(42):e2302780120.

39. Tristan C, Shahani N, Sedlak TW, and Sawa A. The diverse functions of GAPDH: views from different subcellular compartments. Cell Signal. 2011;23(2):317-23.

40. Myers SJ, Malladi CS, Hyland RA, et al. Mutations in the SPTLC1 protein cause mitochondrial structural abnormalities and endoplasmic reticulum stress in lymphoblasts. DNA Cell Biol. 2014;33(7):399-407.

Figure Legends

Figure 1 SPTLC1-related sphingolipid metabolic pathways and the genetic defect in the S331F mouse model. (**A**) SPT catalyses the first step in the synthesis of sphingolipids by conjugating palmitoyl-CoA and L-serine. Mutations in *SPTLC1* reduce the affinity of the

ACCEPTED MANUSCRIPT

Downloaded from https://academic.oup.com/brain/advance-article/doi/10.1093/brain/awaf403/8297247 by DO NOT USE Institute of Education merged with 90002272 user on 29 October 2025

enzyme for L-serine and increase its affinity for alanine and glycine, thereby leading to the formation and accumulation of neurotoxic 1-Deoxy-Sphingoid Bases (DSBs). (**B**) The S331F mouse model carries two heterozygous variants, c.990 C>G and c.992 C>T (p.S331F) in exon 11 of mouse *Sptlc1* gene, generated by CRISPR/Cas9 genome editing. ASOs were designed to target the indicated ASO binding region on the mutant allele at both mRNA and pre-mRNA levels.

Figure 2 ASOs silence the mutant transcripts in skin fibroblasts cultured from S331F mice. Nine ASOs were designed in 2'-OMe, MOE or LNA chemistry, and tested in cultured skin fibroblasts from mice either at 10 nM by (**A**) lipofectamine 2000 transfection or (**B**) at 10 μM by gymnosis. WT and mutant transcripts were quantified by allele-specific qRT-PCR, normalized to the levels of mock or blank controls. Dose-response studies of MOE and LNA-ASOs were performed in mouse fibroblasts treated by (**C**) lipofectamine 2000 transfection in a concentration range of 0 to 50 nM, or (**D**) gymnosis in a concentration range of 0 to 10 μM. The IC50 values of ASOs on the mutant (in red) or WT (in blue) transcripts were measured and indicated.

Figure 3 LNA-ASOs selectively silence the mutant transcripts *in vivo* in the S331F mice. (**A**) Newborn S331F mice at PND3 and (**B**) young adult mice at six weeks old received single subcutaneous (SC) injection of LNA-ASO1 or LNA-ASO3 at 25 μg/g. liver and DRGs were collected at seven days after the injection. WT and mutant (Mut) *Sptlc1* mRNA levels in ASO-treated mice were measured by allele-specific qRT-PCR and normalized to saline control mice. (**C**) The duration of silencing effect in the liver and DRGs in adult mice after a single SC injection of LNA-ASO1 at 25 μg/g was measured at 14 days after the injection, by allele-specific qRT-PCR and normalized to saline control mice. (**D**) Dose-response studies were performed in 6-week-old mice treated with single SC injection of LNA-ASO1 at 10, 15, 20 and 25 μg/g. The allele-specific silencing was measured by qRT-PCR in the liver and DRGs 7 days after the injection. Two-way ANOVA and Sidak's multiple comparisons test were performed for statistical significance. N=3-6 mice/group. *p<0.05, **p<0.01, ***p<0.001, ****p<0.0001. Created in BioRender. Zhou, H. (2025) https://BioRender.com/8css706.

ACCEPTED MANUSCRIPT

Downloaded from https://academic.oup.com/brain/advance-article/doi/10.1093/brain/awaf403/8297247 by DO NOT USE Institute of Education merged with 9000272 user on 29 October 2025

Figure 4 Repeated weekly ASOs treatment selectively silence the mutant transcripts *in vivo* in the S331F mice. (**A**) The timeline of repeated ASO treatment. Four-week-old mice received weekly SC injection of LNA-ASO1, GalNAc-LNA-ASO1 or MOE-ASO1 for 8 weeks. Liver, DRGs and sciatic nerves were collected for allele-specific qRT-PCR one week after the 8th treatment. Blood samples were collected at baseline (4 weeks old), just before the 1st injection, and after 4 weeks and 8 weeks of treatment. (**B**) The silencing effects of LNA-ASO1 and GalNAc-LNA-ASO1 in the liver, DRGs and sciatic nerves after 8-week treatment were measured by allele-specific qRT-PCR. The mutant (Mut) and WT *Sptlc1* mRNA levels were compared between LNA-ASO1, GalNAc-LNA-ASO1 and normalized to saline controls. (**C**) The silencing effects of MOE-ASO1 in the liver, DRGs and sciatic nerves after 8-week treatment were measured by allele-specific qRT-PCR. The mutant (Mut) and WT *Sptlc1* mRNA levels in ASO-treated group were normalized to saline controls. (**D**) The tissue concentrations of ASOs in peripheral organs were measured by SplintR PCR. Two-way ANOVA and Sidak's multiple comparisons test were performed for statistical significance. N=3-8 mice/group. *p<0.05, **p<0.01, ***p<0.001, ****p<0.0001. Created in BioRender. Zhou, H. (2025) https://BioRender.com/j3joxe5.

Figure 5 Plasma levels of 1-deoxySL are increased in the S331F mice and reduced after effective ASO treatment. (**A**) Plasma levels of the neurotoxic 1-deoxySL were increased in the S331F mice compared to WT, measured at postnatal day 7 (D7), 14, 28 and 56. N = 4-13 mice /group/time point. Unpaired Student t test was used for data analysis at each time point. 1-deoxySLs were measured in (**B**) neonatal mice and (**C**) adult mice at 7 days after a single subcutaneous injection of ASOs, and in adult mice received repeated weekly injection of ASOs for 4 weeks (**D**) and 8 weeks (**E**). One-way ANOVA or Kruskal-Wallis, followed by Tukey's or Dunn's tests were performed when appropriate. (F) Comparison of plasma levels of 1-deoxySL between 4 and 8 weeks of different treatment. Two-way ANOVA and Sidak's multiple comparisons test were performed. N= 4-10 mice/group. Results were presented as Mean ± SEM. *p<0.05, **p<0.01, ***p<0.001, ****p<0.0001.

ACCEPTED MANUSCRIPT

Downloaded from https://academic.oup.com/brain/advance-article/doi/10.1093/brain/awaf403/8297247 by DO NOT USE Institute of Education merged with 9000272 user on 29 October 2025

Figure 6 Transcriptomic studies in the S331F mice and its response to ASO treatment. (**A**) *Left*: The top eleven significantly enriched pathways identified in Gene Ontology (GO) enrichment analysis. *Middle*: The top four significant pathways identified in Encyclopedia of Genes and Genomes (KEGG) enrichment analysis. *Right*: The top nine enriched pathways identified by Reactome database enrichment analysis. (**B**) The expression of four selected DEGs, *Mt-Co2, Gapdh, Slc385a* and *Mt-ATP6*, in the DRGs (*top*), and the liver (*bottom*), from male and female mice, respectively. Two-way ANOVA and Sidak's multiple comparisons test were performed. *N*=5-6 mice/group. (**C** and **D**) The expression of *Scl38a5*, *Gapdh, Slc385a* and *Mt-ATP6* in the DRGs (**C**), and the liver (**D**), from WT female mice, S331F female mice treated with saline or different ASOs for 8 weeks. *N*=4-5 mice/group. One-way ANOVA or Kruskal-Wallis, followed by Tukey's or Dunn's tests were performed when appropriate. Data were presented as Mean ± SEM. * $p<0.05$, ** $p<0.01$, *** $p<0.001$, **** $p<0.0001$.

ACCEPTED MANUSCRIPT

Downloaded from https://academic.oup.com/brain/advance-article/doi/10.1093/brain/awaf403/8297247 by DO NOT USE Institute of Education merged with 90002272 user on 29 October 2025

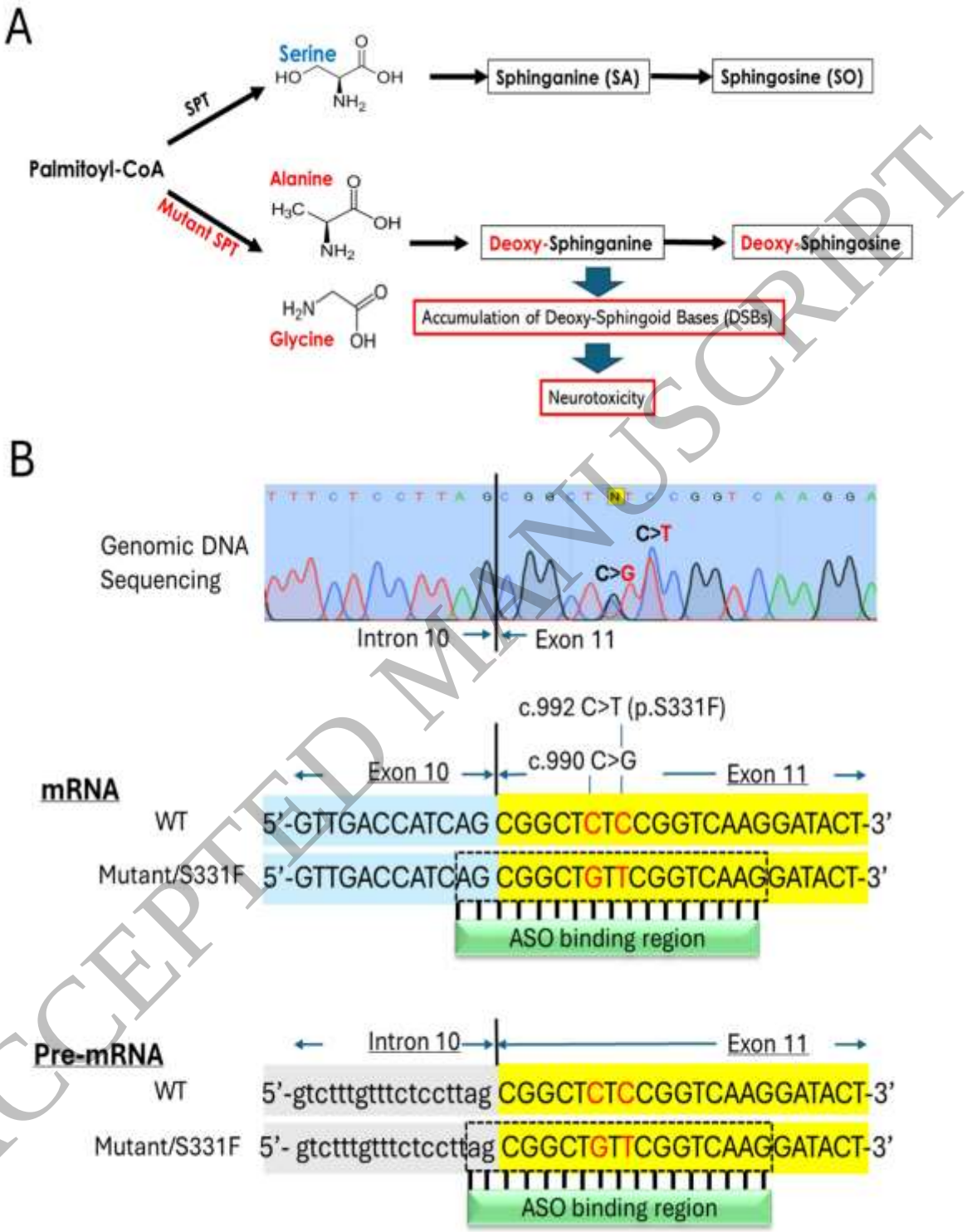

Figure 1
208x234 mm (x DPI)

ACCEPTED MANUSCRIPT

Downloaded from https://academic.oup.com/brain/advance-article/doi/10.1093/brain/awaf403/8297247 by DO NOT USE Institute of Education merged with 9000272 user on 29 October 2025

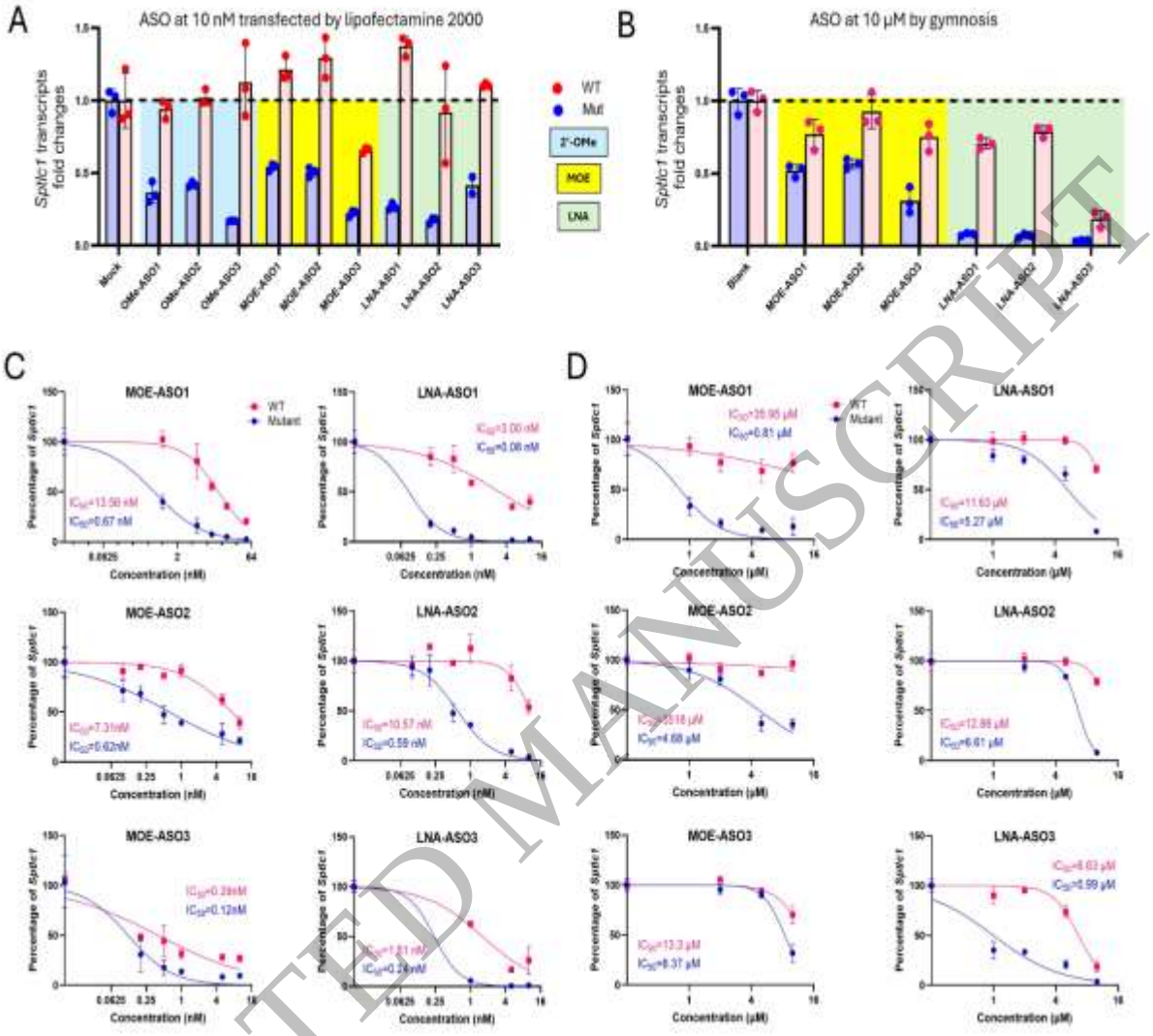

Figure 2
305x226 mm (x DPI)

ACCEPTED MANUSCRIPT

Downloaded from https://academic.oup.com/brain/advance-article/doi/10.1093/brain/awaf403/8297247 by DO NOT USE Institute of Education merged with 9000272 user on 29 October 2025

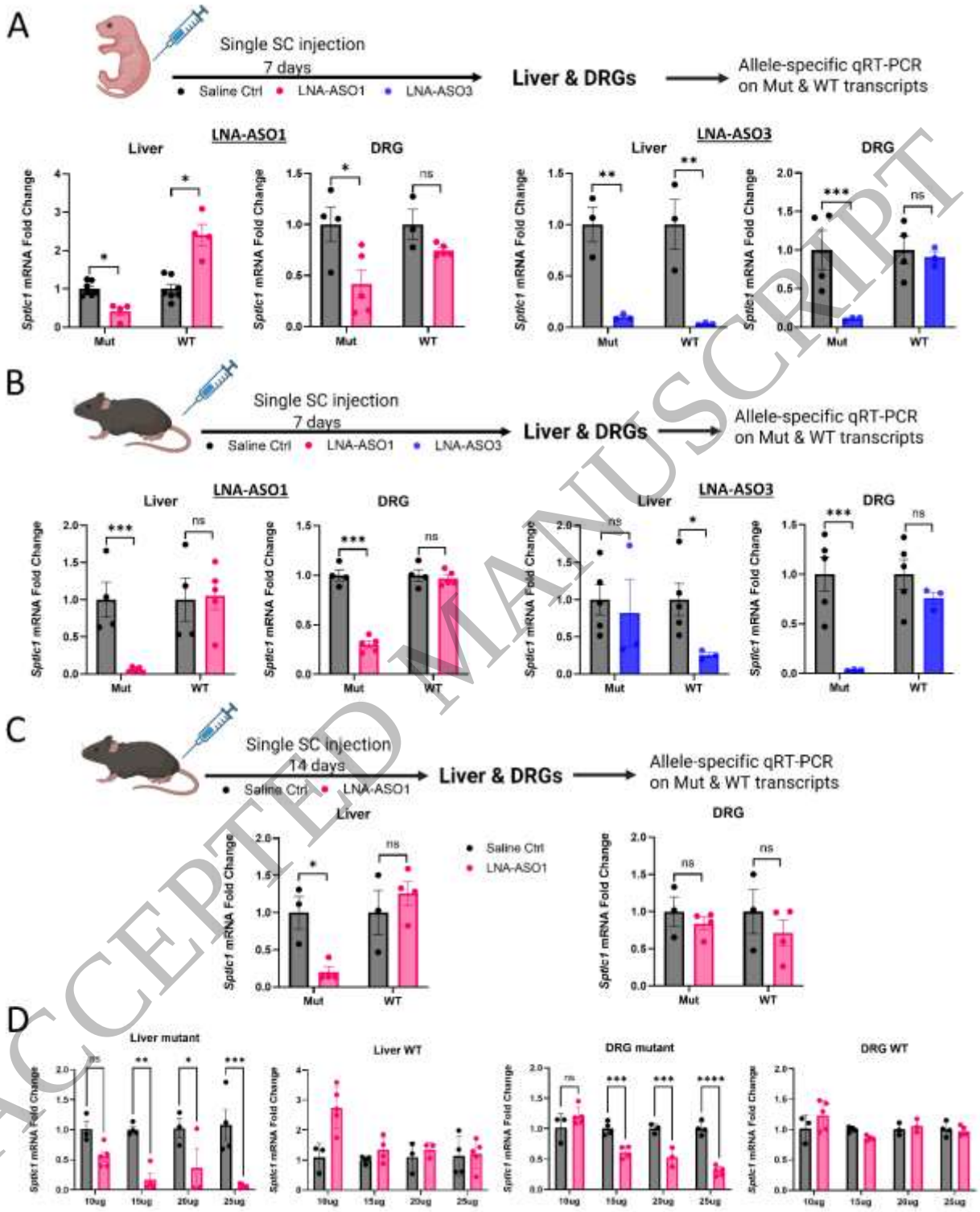

Figure 3
322x402 mm (x DPI)

ACCEPTED MANUSCRIPT

Downloaded from https://academic.oup.com/brain/advance-article/doi/10.1093/brain/awaf403/8297247 by DO NOT USE Institute of Education merged with 9000272 user on 29 October 2025

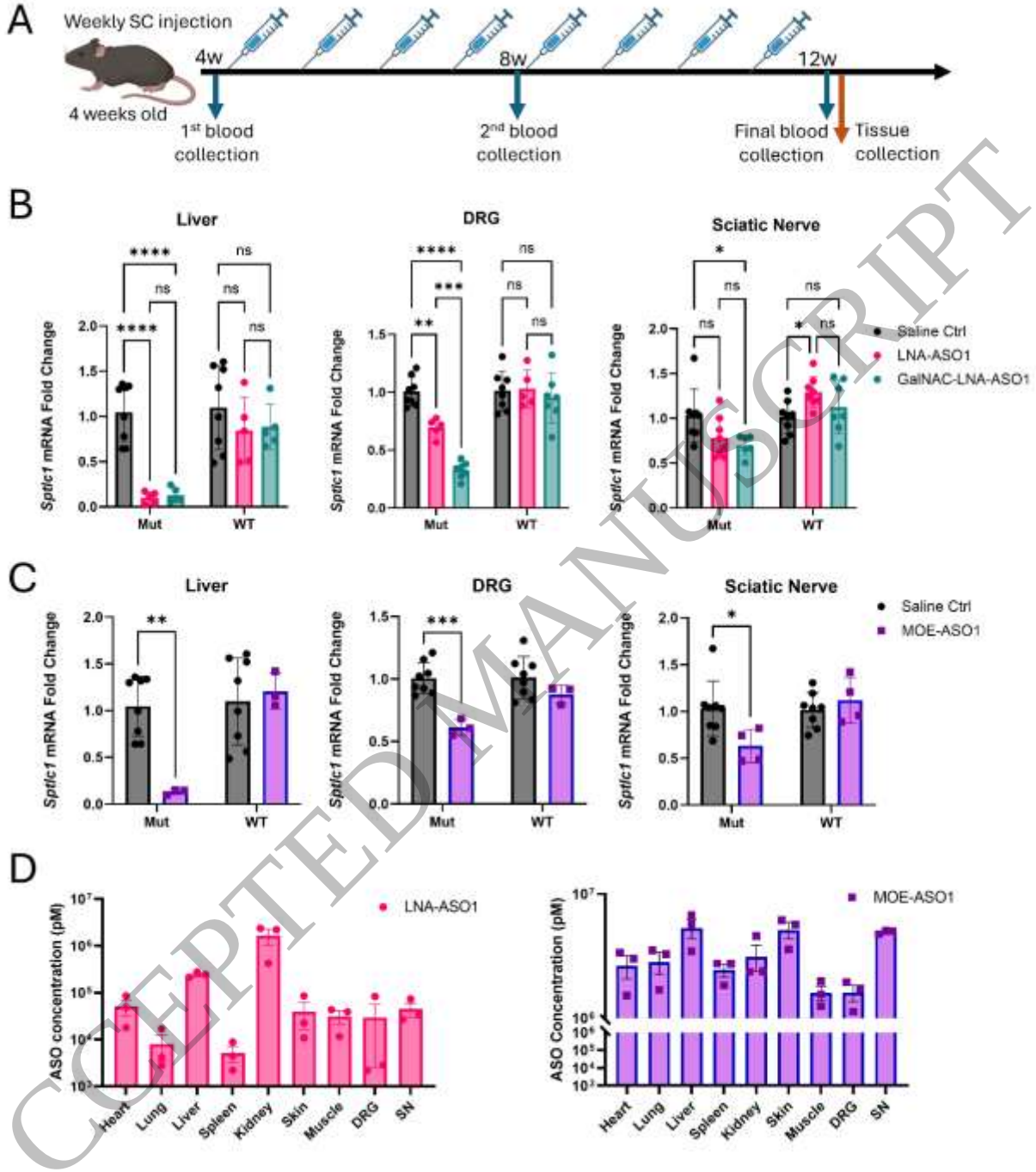

Figure 4
307x340 mm (x DPI)

ACCEPTED MANUSCRIPT

Downloaded from https://academic.oup.com/brain/advance-article/doi/10.1093/brain/awaf403/8297247 by DO NOT USE Institute of Education merged with 9000272 user on 29 October 2025

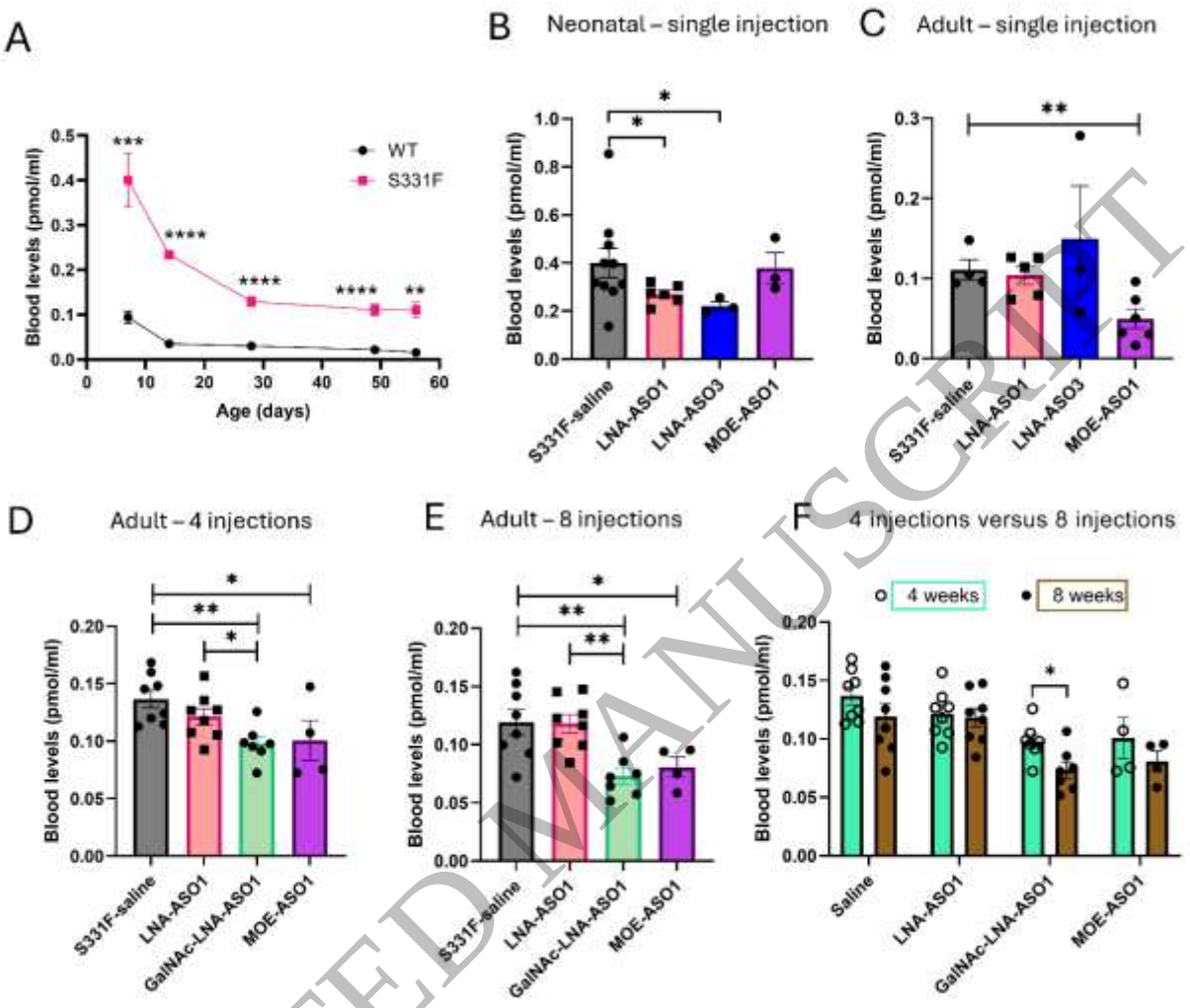

Figure 5
385x327 mm (x DPI)

ACCEPTED MANUSCRIPT

Downloaded from https://academic.oup.com/brain/advance-article/doi/10.1093/brain/awaf403/8297247 by DO NOT USE Institute of Education merged with 9000272 user on 29 October 2025

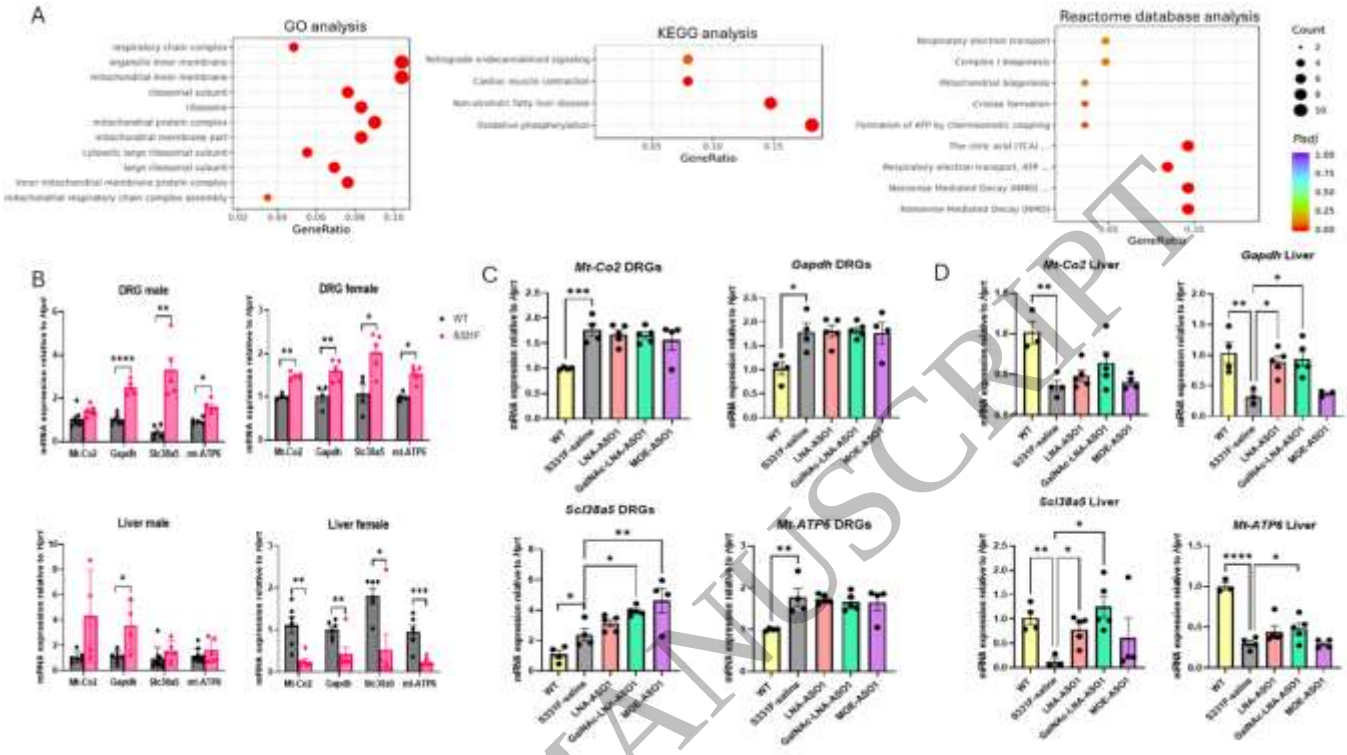

Figure 6
185x107 mm (x DPI)

Table 1 The list of ASOs tested in this study

ID	Chemistry	ASO sequence	Length (Mer)
OMe-ASO1	2'-OMe	[UUGA]C*C*G*A*A*C*A*G*C*[CGCU]	17
OMe-ASO2	2'-OMe	[UUGA]C*C*G*A*A*C*A*G*C*C*[GCU]	17
OMe-ASO3	2'-OMe	[CUUG]A*C*C*G*A*A*C*A*G*C*[CGCU]	18
MOE-ASO1	MOE	<UUGA>C*C*G*A*A*C*A*G*C*<CGCU>	17
MOE-ASO2	MOE	<UUGA>C*C*G*A*A*C*A*G*C*C*<GCU>	17
MOE-ASO3	MOE	<CUUG>A*C*C*G*A*A*C*A*G*C*<CGCU>	18
LNA-ASO1	LNA	{UUGA}C*C*G*A*A*C*A*G*C*{CGCU}	17
LNA-ASO2	LNA	{UUGA}C*C*G*A*A*C*A*G*C*C*{GCU}	17
LNA-ASO3	LNA	{CUUG}A*C*C*G*A*A*C*A*G*C*{CGCU}	18

ASO- antisense oligonucleotide; Phosphorothioate (PS)-modified DNA nucleotides are indicated with an asterisk; RNA nucleotides modified with 2'-*O*-methyl (2'-OMe) chemistry are included in square brackets; RNA nucleotides modified with 2'-*O*-methoxy ethyl (MOE) chemistry are included in angle brackets; RNA nucleotides modified with locked nucleic acid (LNA) chemistry are included in curly brackets. Nucleotides complementary to c.990G and c.992T are underlined.

ACCEPTED MANUSCRIPT

Downloaded from https://academic.oup.com/brain/advance-article/doi/10.1093/brain/awaf403/8297247 by DO NOT USE Institute of Education merged with 90002272 user on 29 October 2025